

HEMBLIP: A VISION–LANGUAGE MODEL FOR INTERPRETABLE LEUKEMIA CELL MORPHOLOGY ANALYSIS

Julie van Logtestijn¹ Petru Manescu¹

¹Department of Computer Science, University College London, United Kingdom

ABSTRACT

Microscopic evaluation of white blood cell morphology is central to leukemia diagnosis, yet current deep learning models often act as black boxes, limiting clinical trust and adoption. We introduce HemBLIP, a vision–language model designed to generate interpretable, morphology-aware descriptions of peripheral blood cells. Using a newly constructed dataset of $\sim 14k$ healthy and leukemic cells paired with expert-derived attribute captions, we adapt a general-purpose VLM via both full fine-tuning and LoRA-based parameter-efficient training, and benchmark against the biomedical foundation model MedGEMMA. HemBLIP achieves higher caption quality and morphological accuracy, while LoRA adaptation provides further gains with significantly reduced computational cost. These results highlight the promise of vision–language models for transparent and scalable hematological diagnostics.

Index Terms— Vision–language models, explainable AI, leukemia diagnosis, hematology, morphological analysis, parameter-efficient fine-tuning

1. INTRODUCTION

Leukemia remains a major global health concern, responsible for around 2.5% of all new cancer diagnoses and 3.1% of cancer deaths worldwide [1]. Despite advances in therapy, the disease continues to impose substantial burden even in high-income countries, with an incidence of roughly 14 per 100,000 and a mortality rate near 6 per 100,000 per year [2]. In low- and middle-income regions, survival rates can drop below 30%, largely due to delayed or missed diagnoses linked to workforce shortages and limited laboratory infrastructure [3, 4, 5].

Leukemia diagnosis relies on microscopical examination of peripheral blood smears (PBS) and bone marrow aspirates (BMA) by hematologists [6]. Morphological cues such as nuclear shape, chromatin texture, nucleoli, and cytoplasmic features are used to classify major subtypes—acute lymphoblastic (ALL), acute myelogenous (AML), chronic lymphocytic (CLL), and chronic myelogenous (CML) [7]. However, this process is labor-intensive, prone to human errors, and requires the availability of trained experts [8].

Recent studies have demonstrated the potential of deep learning vision models to detect leukemic cells in PBS and BMA [9, 10]. However, these task-specific classifiers often require frequent retraining when imaging conditions, staining protocols, or cell morphology distributions vary, which is difficult to sustain in real-world and low-resource settings [11, 12]. More critically, their black-box outputs typically provide only class predictions without articulating the morphological reasoning behind them. This lack of interpretability limits clinical trust, validation, and ultimately adoption in routine hematology workflows [13, 14].

Here, we propose an explainable-by-design computational hematology approach underpinned by Vision Language Models (VLM) capable of generating narrative descriptions of cells from PBS and BMA. By jointly learning from images and text, VLMs associate visual patterns with descriptive language, enabling tasks such as image captioning and visual question answering [15]. Recent studies have shown that VLMs can be trained to generate full radiology reports and draft histopathology narratives directly from gigapixel slides [16, 17]. We present HemBLIP, a vision–language modeling approach designed to generate morphology-aware descriptions of white blood cells in the context of leukemia diagnosis from blood film microscopy. We trained our model on a newly constructed morphology-rich dataset of $\sim 14k$ cell–caption pairs and compared its performance with a medical foundation model (MedGEMMA) under full and Low-Rank Adaptation (LoRA) fine-tuning.

2. MATERIALS AND METHODS

2.1. Dataset Construction

We composed a morphology-aware dataset of peripheral blood smear images combining healthy and leukemic white blood cells (WBCs). For healthy cells, we used the *WB-CAtt dataset* [18], containing 10k expert-annotated WBCs (neutrophils, eosinophils, basophils, lymphocytes, monocytes) with 11 categorical attributes describing nuclear, cytoplasmic, and granular features. For leukemia, we used the *LeukemiaAtrri dataset* [19], which provides 10k labeled cells across five subtypes (ALL, AML, APML, CLL, CML) and seven expert-defined morphological attributes (e.g., chro-

matin texture, nucleoli visibility, basophilia). After filtering incomplete or erroneous entries, we selected 7,037 healthy and 7,622 leukemic cells.

We further paired each cell image with a structured natural-language caption describing its morphology. Feature labels were transformed into templated sentences and augmented with GPT-4 paraphrases while constraining generation to retain factual morphological descriptors and diagnostic labels. The resulting corpus comprises $\sim 14k$ image–text pairs covering normal and leukemic morphologies. Figure 2 illustrates two sample images and ground truth generated captions.

2.2. Model Architectures and Fine-tuning

We propose HemBLIP, a vision–language model adapted from the general-purpose BLIP architecture [20] for the task of white blood cell morphology captioning. HemBLIP couples a ViT-based image encoder with a transformer text decoder and is fine-tuned to generate structured, clinically meaningful cell descriptions. To achieve efficient domain adaptation, we apply Low-Rank Adaptation (LoRA) [21] to the decoder attention layers while keeping the vision encoder frozen, enabling morphology-aware learning without extensive retraining. We additionally evaluate a fully fine-tuned HemBLIP variant to examine the trade-offs between parameter-efficient and full adaptation strategies. To contextualize performance, we compared HemBLIP against a biomedical foundation model, MedGEMMA-4B [22], which combines a SigLIP vision tower with a medically aligned language decoder trained on diverse clinical image–text data. Model architectures are summarized in Figure 1. All models were optimized using AdamW (learning rate 5×10^{-5}) with early stopping based on validation loss. The implementation is available at: <https://github.com/julievanlogtestijn-ncl/Vision-Language-Models-for-Leukemia-Detection/>.

2.3. Clinical Relevance Evaluation

Standard captioning metrics such as BLEU, ROUGE-L, and BERTScore [23, 24] were computed to assess lexical and semantic similarity with reference captions. To quantify morphological faithfulness, we developed a regex-based attribute extractor that performs controlled string matching over generated captions to identify mentions of predefined cytological attributes (e.g., cell size, chromatin pattern, nucleoli, basophilia). Extracted attributes were compared to ground-truth labels, and confusion matrices were used to evaluate correspondence and categorize biologically plausible errors (e.g., coarse vs. open chromatin, small vs. medium cell size).

To probe whether models encode diagnostically meaningful visual information, we trained lightweight cosine-similarity classifier heads on frozen image embeddings to distinguish between leukemia subtypes and cell types.

2.4. External Validation

An additional set of 507 cell images from the Blood Cell Atlas [25], a public Kaggle collection [26], and the low-cost microscope subset of the *LeukemiaAttri dataset* [19] was used for robustness testing under domain shift. These samples include both healthy and malignant cells imaged under varied staining and sensor conditions, allowing evaluation of real-world generalization.

3. RESULTS

We evaluated captioning performance, morphological interpretability, and representation quality across internal and external test sets. Example model outputs are shown in Fig. 2.

3.1. Caption Generation Performance

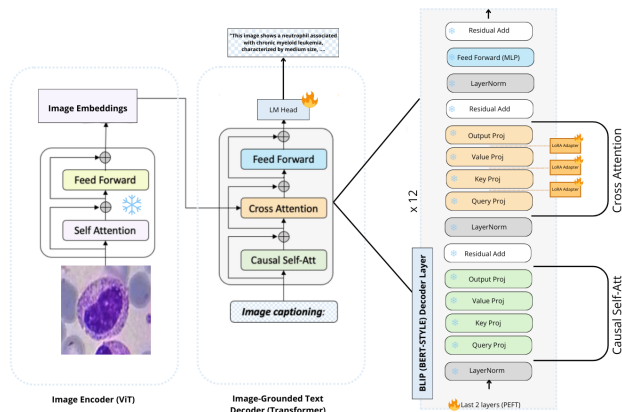
Table 1 reports quantitative caption generation metrics on both test sets. LoRA-adapted models consistently outperform their fully fine-tuned or base counterparts, confirming the benefits of parameter-efficient adaptation. The domain-specialized *MedGEMMA LoRA* achieves the strongest internal metrics (BLEU 0.31, ROUGE-L 0.52, BERTScore 0.87), while *HemBLIP LoRA* achieves comparable results with notably lower computational cost. Under external validation, both LoRA variants retain higher semantic alignment (ROUGE-L 0.25, BERTScore 0.78) than their base models, highlighting improved robustness to microscope and staining variations.

Table 1: Caption generation metrics on internal and external test sets.

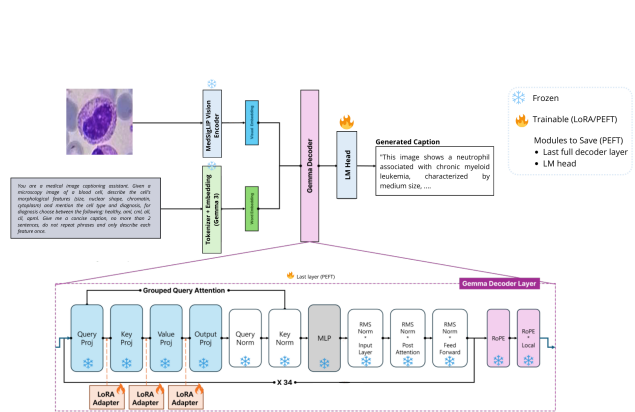
Model	Internal			External		
	BLEU	ROUGE-L	BERTScore F1	BLEU	ROUGE-L	BERTScore F1
HemBLIP Full	0.24	0.42	0.83	0.02	0.22	0.77
HemBLIP LoRA	0.27	0.49	0.86	0.02	0.25	0.78
MedGEMMA Base	0.02	0.13	0.74	0.02	0.18	0.74
MedGEMMA LoRA	0.31	0.52	0.87	0.02	0.23	0.77

3.2. Morphological Attribute Accuracy

To assess the relevance of descriptions, we extracted key morphological attributes (e.g., cell size, chromatin texture, nuclear shape) from generated captions using a regex-based evaluator. As shown in Table 2, HemBLIP models consistently produced more accurate and clinically relevant morphological attributes than MedGEMMA variants, both internally and externally. While LoRA fine-tuning yielded only minor gains over full HemBLIP, it provided comparable performance at substantially lower training cost. All models exhibited expected degradation under external evaluation, reflecting domain shift effects.



(a) BLIP architecture overview. The ViT-based vision encoder and transformer text decoder are aligned through contrastive and captioning objectives.



(b) MedGEMMA architecture overview. A SigLIP vision tower is coupled with a medically tuned decoder trained on multimodal clinical data.

Fig. 1: Comparison of the two vision–language architectures used in this study. Both were fine-tuned on the morphology-aware leukemia dataset using LoRA adapters for parameter-efficient adaptation.

Table 2: Feature-level accuracy (%) for morphological attributes extracted from generated captions on internal and external test sets. Only frequently mentioned features are shown.

Feature	HemBLIP Full		HemBLIP LoRA		MedGEMMA Base		MedGEMMA LoRA	
	Int.	Ext.	Int.	Ext.	Int.	Ext.	Int.	Ext.
Cell type	73.26	38.60	72.40	29.58	14.70	7.93	57.73	22.45
Nuclear chromatin texture	52.72	32.41	55.47	31.12	51.93	42.59	59.30	31.36
Cytoplasm amount	70.35	50.23	69.87	43.91	26.67	0.00	57.37	35.99
Diagnosis	79.14	43.45	82.27	53.85	16.96	21.74	54.09	41.03
Nuclear shape	77.38	7.91	72.90	14.25	56.62	65.68	64.22	12.06
Overall shape	77.44	11.46	77.68	15.78	61.79	14.99	75.80	17.79
Cell size	91.80	47.78	85.37	41.07	32.33	19.90	81.15	31.23

3.3. HemBLIP as a feature extractor

Finally, we evaluated whether visual encoders captured discriminative morphology by training lightweight classifiers on frozen embeddings from each backbone. Since LoRA fine-tuning did not modify the vision encoders, this comparison focuses on the *HemBLIP Full* model (fully fine-tuned, including the vision tower), the original *BLIP Base*, the *MedGEMMA* backbone, and a random projection baseline.

As shown in Table 3, HemBLIP Full achieved the strongest performance for both leukemia subtype (Acc. 0.85, F1 0.83; 5 classes) and cell-type classification (Acc. 0.60, F1 0.64; 13 classes), outperforming MedGEMMA and baseline embeddings. External test performance dropped substantially (Acc. 0.52 / 0.33), highlighting ongoing challenges in domain generalization. These findings suggest that full HemBLIP fine-tuning yields visual representations that retain clinically

meaningful diagnostic cues beyond caption generation.

Table 3: Frozen-backbone classifier performance on internal and external test sets. Accuracy and weighted F1 scores are reported for leukemia subtype and cell-type classification.

Task	Backbone	Internal		External	
		Acc.	F1	Acc.	F1
Leukemia subtype	HemBLIP Full	0.848	0.834	0.517	0.474
	BLIP Base	0.807	0.804	0.501	0.516
	MedGEMMA	0.708	0.713	0.456	0.474
Cell type	HemBLIP Full	0.595	0.644	0.330	0.363
	BLIP Base	0.520	0.570	0.151	0.183
	MedGEMMA	0.344	0.353	0.117	0.132

Ground Truth Caption	Model Generated Caption
	<ul style="list-style-type: none"> • BLIP base: an image of a purple substance • BLIP Full: in this case of healthy, an eosinophil is visible with distinct morphological features. • BLIP LoRA: in this case of healthy, an eosinophil is visible with distinct morphological features. • MedGEMMA base: The image shows a blood smear with a cluster of abnormal cells, likely indicating a hematological disorder. • MedGEMMA LoRA: A representative image of an eosinophil with features such as small size, round overall shape, segmented-blobbed nucleus, low nuclear-to-cytoplasmic ratio, densely chromatin, clear cytoplasmic texture, light blue cytoplasm, round red granules.
	<ul style="list-style-type: none"> • BLIP base: a purple spherules score • BLIP Full: neutrophil observed in a case of chronic myeloid leukemia. Notable features include medium size, regular nuclear shape, open nuclear chromatin, inconspicuous nucleolus, abundant cytoplasm, slight basophilia. • BLIP LoRA: this is a neutrophil from a chronic myeloid leukemia case, noted for its medium size, regular nuclear shape, coarse nuclear chromatin, inconspicuous nucleolus, abundant cytoplasm, slight basophilia. • MedGEMMA base: This image shows a stained blood cell, likely a lymphocyte, with a circular shape and a distinct nucleus. • MedGEMMA LoRA: In this case of chronic myeloid leukemia, a neutrophil is visible with distinct morphological features. Notable features include medium size, regular nuclear shape, coarse nuclear chromatin, inconspicuous nucleolus, abundant cytoplasm, slight basophilia.

Fig. 2: Example blood cell inputs with ground-truth captions and model-generated descriptions. Each model exhibits varying degrees of morphological specificity and diagnostic accuracy.

4. CONCLUSION

This work presented an explainable AI framework for leukemia diagnosis from blood films using vision–language models. By constructing a morphology-rich dataset that combines expert annotations with GPT-generated captions, we enable models to learn descriptive reasoning aligned with hematological practice. Using parameter-efficient LoRA fine-tuning, both a general-domain model (BLIP) and a biomedical model (MedGEMMA) were adapted to generate morphology-aware captions and diagnostic labels.

Our results show that LoRA adaptation not only reduces computational cost but also improves the clinical relevance of generated explanations. Our HemBLIP model produced the most accurate and interpretable descriptions, demonstrating that general-purpose VLMs can be successfully repurposed for specialized medical images. The proposed evaluation pipeline—linking textual outputs to morphological attributes and testing discriminative power—provides a practical approach to assess explainability in medical AI.

Overall, this study highlights how morphology-aware VLMs can bridge the gap between automated image analysis and human interpretability, offering a scalable path toward transparent, clinically useful AI-assisted leukemia diagnostics.

5. ACKNOWLEDGMENTS

No funding was received for conducting this study. The authors have no relevant financial or non-financial interests to disclose.

6. COMPLIANCE WITH ETHICAL STANDARDS

This research did not involve any studies with human participants or animals performed by any of the authors. The study used only publicly available datasets; therefore, ethical approval was not required.

7. REFERENCES

- [1] Hyuna Sung, Jacques Ferlay, Rebecca L. Siegel, Mathieu Laversanne, Isabelle Soerjomataram, Ahmedin Jemal, and Freddie Bray, “Global Cancer Statistics 2020: GLOBOCAN Estimates of Incidence and Mortality Worldwide for 36 Cancers in 185 Countries,” *CA: A Cancer Journal for Clinicians*, vol. 71, no. 3, pp. 209–249, 2021.
- [2] National Cancer Institute, “SEER Cancer Stat Facts: Leukemia,” <https://seer.cancer.gov/statfacts/html/leuks.html>, Age-adjusted incidence and mortality rates. Accessed 2025-08-27.
- [3] Nickhill Bhakta, Lisa M. Force, Claudia Allemani, Rifat Atun, Freddie Bray, Michel P. Coleman, Eva Steliarova-Foucher, A. Lindsay Frazier, Leslie L. Robison, Carlos Rodriguez-Galindo, and Christina Fitzmaurice, “Childhood cancer burden: a review of global estimates,” *Lancet Oncology*, vol. 20, no. 1, pp. e42–e53, 2019.
- [4] Shahin Sayed, Robert Lukande, and Kenneth A. Fleming, “Providing pathology support in low-income countries,” *Journal of Global Oncology*, vol. 1, no. 1, pp. 3–6, 2015.
- [5] C. De Angelis, C. Pacheco, G. Lucchini, M. Arguello, V. Conter, A. Flores, A. Biondi, G. Masera, and F. Baez, “The experience in nicaragua: Childhood leukemia in low income countries—the main cause of late diagnosis may be ”medical delay,”” *International Journal of Pediatrics*, vol. 2012, pp. 129707, 2012.
- [6] Mithraa Devi Sekar, Manasa Raj, and Prabhu Manivannan, “Role of Morphology in the Diagnosis of Acute Leukemias: A Systematic Review,” *Indian Journal of Medical and Paediatric Oncology*, vol. 44, no. 4, pp. 464–473, 2023.
- [7] A. S. Davis, A. J. Viera, and M. D. Mead, “Leukemia: An overview for primary care,” 2014.
- [8] M. M. Amin, S. Kermani, A. Talebi, and M. G. Oghli, “Recognition of acute lymphoblastic leukemia cells in microscopic images using k-means clustering and support vector machine classifier,” *Journal of Medical Signals and Sensors*, vol. 5, no. 1, pp. 49–58, Jan–Mar 2015.
- [9] Sajida Perveen, Abdullah Alourani, Muhammad Shahbaz, M. Usman Ashraf, and Isma Hamid, “A framework for early detection of acute lymphoblastic leukemia and its subtypes from peripheral blood smear images using deep ensemble learning technique,” *IEEE Access*, vol. 12, pp. 29252–29268, 2024.

[10] Geng Yan, Gao Mingyang, Shi Wei, Liang Hongping, Qin Liyuan, Liu Ailan, Kong Xiaomei, Zhao Huilan, Zhao Juanjuan, and Qiang Yan, “Diagnosis and typing of leukemia using a single peripheral blood cell through deep learning,” *Cancer Science*, vol. 116, no. 2, pp. 533–543, 2025.

[11] Connor Shorten and Taghi M. Khoshgoftaar, “A survey on image data augmentation for deep learning,” *Journal of Big Data*, vol. 6, no. 1, pp. 60, 2019.

[12] Ming Lu, Wei Chen, Ji Chen, et al., “Dataset bias in medical imaging ai: an emerging challenge,” *NPJ Digital Medicine*, vol. 5, no. 1, pp. 134, 2022.

[13] Amina Adadi and Mohamed Berrada, “Peeking inside the black-box: A survey on explainable artificial intelligence (XAI),” *IEEE Access*, vol. 6, pp. 52138–52160, 2018.

[14] Andreas Holzinger, Georg Langs, Harald Denk, Kurt Zatloukal, and Hermann Müller, “Causability and explainability of artificial intelligence in medicine,” *Wiley Interdisciplinary Reviews: Data Mining and Knowledge Discovery*, vol. 9, no. 4, pp. e1312, 2019.

[15] Akash Ghosh, Arkadeep Acharya, Sriparna Saha, Vinija Jain, and Aman Chadha, “Exploring the frontier of vision-language models: A survey of current methodologies and future directions,” *arXiv preprint arXiv:2404.07214*, 2024.

[16] Ryutaro Tanno, David GT Barrett, Andrew Sellergren, Sumedh Ghaisas, Sumanth Dathathri, Abigail See, Johannes Welbl, Charles Lau, Tao Tu, Shekoofeh Azizi, et al., “Collaboration between clinicians and vision-language models in radiology report generation,” *Nature Medicine*, vol. 31, no. 2, pp. 599–608, 2025.

[17] Manuel Tran, Paul Schmidle, Ruifeng Ray Guo, Sophia J Wagner, Valentin Koch, Valerio Lupperger, Brenna Novotny, Dennis H Murphree, Heather D Hardway, Marina D’Amato, et al., “Generating dermatopathology reports from gigapixel whole slide images with histogpt,” *Nature Communications*, vol. 16, no. 1, pp. 4886, 2025.

[18] Satoshi Tsutsui, Winnie Pang, and Bihan Wen, “WB-CAtt: A white blood cell dataset annotated with detailed morphological attributes,” *Advances in Neural Information Processing Systems (NeurIPS) 36*, pp. 50796–50824, 2023.

[19] Abdul Rehman, Talha Meraj, Aiman Mahmood Minhas, Ayisha Imran, Mohsen Ali, and Waqas Sultani, “A large-scale multi domain leukemia dataset for the white blood cells detection with morphological attributes for explainability,” *arXiv preprint arXiv:2405.10803v1*, 2024.

[20] Junnan Li, Dongxu Li, Caiming Xiong, and Steven Hoi, “Blip: Bootstrapping language-image pre-training for unified vision-language understanding and generation,” 2022.

[21] Edward J Hu, Yelong Shen, Phillip Wallis, Zeyuan Allen-Zhu, Yuanzhi Li, Shean Wang, Lu Wang, Weizhu Chen, et al., “Lora: Low-rank adaptation of large language models,” *ICLR*, vol. 1, no. 2, pp. 3, 2022.

[22] Andrew Sellergren, Sahar Kazemzadeh, Tiam Jaroensri, Atilla Kiraly, Madeleine Traverse, Timo Kohlberger, Shawn Xu, and et al., “Medgemma technical report,” 2025.

[23] Tianyi Zhang, Varsha Kishore, Felix Wu, Kilian Q. Weinberger, and Yoav Artzi, “Bertscore: Evaluating text generation with bert,” 2020.

[24] Jinhyuk Lee, Wonjin Yoon, Sungdong Kim, Donghyeon Kim, Sunkyu Kim, Chan Ho So, and Jaewoo Kang, “Biobert: a pre-trained biomedical language representation model for biomedical text mining,” *Bioinformatics*, vol. 36, no. 4, pp. 1234–1240, 2020.

[25] Shenzhen Mindray Bio-Medical Electronics Co., Ltd., *Blood Cell Atlas*, 2022, Clinical resource.

[26] Sumith Singh Kothwal, “Blood cell images for cancer detection,” 2025, Accessed: 2025-08-26.